SELECTION OF OPTIMUM HEAT EXCHANGER IN DUAL GAS TURBINE COMBINED CYCLES

Taha A. Ellabib, Elhadi I. Dekam*, Bashir A. Aburwin*, Mohammed E. Mashena*

Military Industries Organization, Tarhuna, Libya, *ME Dept. University of Tripoli, Libya.
Email: tahalabib@yaho.com, e.dekam@uot.edu.ly, m.mashena@uot.edu.ly,

الملخص

يدرس هذا البحث المبادل الحراري المثبت بين دورة الغاز العلوية ودورة الهواء السفلية في ضوء خصائص وأداء وتحسين جوانب تصميم دورة محطات توليد القوى. تم التحقيق في أداء دورة القوى المزدوجة مع المبادل الحراري في ظل ظروف تشغيل مختلفة لأنواع وترتيبات متعددة من هذه المبادلات الحرارية المتاحة. تم تقديم نماذج رياضية مختلفة بما في ذلك الشكل الهندسي والتشغيل والأداء والاقتصاد. تم العمل على العديد من الارتباطات العددية لتحويل البيانات المنشورة في الأدبيات إلى علاقات رياضية اقتصادية حرارية. تم إنشاء حزمة برامج كمبيوتر لتنفيذ عمليات التقييم والتصميم والتحسين. تم استخدام مبادلات حرارية، سطح ريش ذات ألواح مسطحة 2.0 مع موائع غير مختلطة لكل ترتيبات التدفق المتقاطع والمعاكس، في حين يتم توظيف توربينين غازيين من وستنق هاوس بقدرة 160 و 32.2 ميجاوات، ينقلان غازات العادم 435 كجم/ثانية و199 كجم/ثانية من الهواء، على التوالي.

تنظر الدراسة في الدورات البسيطة، الدورات مع مبرد داخلي بيني واحد، أو مع اثنين من المبردات الداخلية البينية. تم تحقيق نتائج تفصيلية لدراسة تأثير المعاملات المختلفة والتحسين. هناك علاقة خطية بين فعالية المبادل الحراري معاكس التدفق وكفاءة دورة قوى المحطة، بمعدل كل تحسن في الفعالية بمقدار 0.1 يعطي زيادة بنسبة 1.25٪ في الكفاءة. بالنسبة لمبادلات بأسطح ريش ذات ألواح مسطحة 2.0 مع ترتيب تدفق معاكس، عند الخط الأمثل، يتحسن صافي التوفير إلى 30 و 54٪، لمحطات تحتوي على واحد واثنين من المبردات الداخلية البينية، على التوالي، استنادًا إلى الحالة البسيطة بتكلفة 2.7 مليون دولارًا أمريكيًا. هذا المبادل الحراري المعزز بمبردين داخليين في الدورة، من خلال أبعاد 1.77م × 5.03م × 10.06م، هو الأمثل، مع تحقيق أعلى وفرات في الطاقة والكفاءة والفعالية، مع توفير صاف للطاقة يبلغ 4.1 مليون دولارًا أمريكيًا بكتلة مقدارها 136 طن.

ABSTRACT

This paper studies the desired heat exchanger located between the gas topping cycle and air bottoming cycle in sight of characteristics, performance, and optimizing design aspects among the plant power generation cycle. The performance of the combined power cycle with the desired heat exchanger is investigated under different operating conditions for different available types and arrangements of such heat exchangers. Various mathematical models including geometry, operation, performance, and economy are introduced. Several numerical correlations are worked on to transform the literature published data to thermoeconomic mathematical relationships. Our own computer software package is established to carry out the evaluation, design, and optimization processes. The Plain plate-fin surface 2.0 heat exchangers are employed with unmixed fluids for each cross-flow and counter-flow arrangements, while two Westinghouse gas turbines of 160 and 32.2 MW, are implemented, transporting 435 kg/s flue gases and 199 kg/s air, respectively.

The study considers simple cycles, cycles with one intercooler, or with two intercoolers. Various and detailed parametric, and optimization study outcomes are

achieved. There is a linear relation among counter-flow heat exchanger effectiveness and plant power cycle efficiency, with a rate of each 0.1 effectiveness improvement gives 1.25 % rise in the efficiency. For Plain Plate-Fin Surface 2.00, counter-flow arrangement, at the optimum line, the net savings grow up to 30 and 54%, for plants with one and two intercoolers, respectively, based on the simple case with 2.7 MUSD. This heat exchanger augmented with two intercoolers in the cycle, through dimensions of 1.77 m x 5.03 m x 10.06 m, is the optimum one, has the highest energy savings, efficiency, and effectiveness, with net energy savings of 4.1 MUSD and mass of 136 Ton.

KEYWORDS: Air Bottoming Cycles; Compact Heat Exchangers; Gas Topping Cycle; Plain Plate-Fin Surface Types.

INTRODUCTION

In the power generation processes, there is a need to cut the emissions of CO_2 and to minimize the energy conversion cost, Anheden [1] and Hepperle [2]. The cogeneration combined cycles in power plants are proven to be one of the potential techniques to maintain the quality and accessibility of energy production while reducing exhaust flue gas emissions and cutout fuel consumption, leading to energy conservation and higher energy efficiency, Özgirgin [3]. One of the forms of the combined cycles is the dual gas turbine combined cycle (DGTCC) which adopts an air bottoming cycle (ABC) instead of the conventional steam bottoming cycle (SBC), where many studies and researches have been conducted. Here, the expected huge heat exchanger is one of the main cycle components, carrying out the heat transfer process between the exhausted hot gases and the compressed atmospheric air. The ABC is an alternative promising way to recover exhaust waste thermal energy. Two Brayton cycles can be combined by an air–gas heat exchanger, where the working fluid air is heated via the desired heat exchanger with exhaust heat from the gas turbine topping cycle.

While such cycles are not quite as efficient as steam-gas combined cycles, the ABC combined cycle involving much simplicity, more rugged, and much expected less cost to build, operate and maintain, while it could be developed, commercialized, and installed much rapidly, Williams et al. [4].

The use of air bottoming with small topping gas turbines offers an increase in power and efficiency, Korobitsyn [5], while intercooling is an improvement made in the gas turbine to increase the network obtained from the cycle by decreasing the compressor work without changing the turbine output work, Bathie [6], and also, improves the thermal efficiency, air rate and work ratio, Bejan et al. [7]. This is accomplished by employing multi-stage compression and intercooling processes between every two stages. The advantages of such cycles are obvious include, the absence of water treatment processes, much less cost to build, less to operate and maintain, with relatively compact dimensions.

The thermal heat exchange processes through heat exchangers are playing a significant role in the combined power cycles, Incropera et al. [8]. These heat exchangers have a great variety due to type of applications, design techniques, and quality of equipment. They are classified according to transfer process, number of fluids, and heat transfer mechanisms, while there are other classifications depend on the heat transfer surface area per volume ratio, construction type, compactness, and flow arrangements, Kreith et al. [9], Cengel [10], and Kupprn [11]. The heat can be transferred by direct contact of fluids, or across the intermediate walls. Here, the two gases do not mix, where the clean air keeps its identity, enabling its usage with minimum environmental impact.

Compact heat exchangers are the desired ones for such present topic, where the surface heat transfer area density is greater than 700 m^2/m^3, having low heat transfer coefficients, while weight and size are important issues, shah [12]. Numerous types use special enhancement techniques to achieve the required heat transfer in smaller plot areas, where the core is one of the main fundamental compact exchanger elements, consists of a pair of parallel plates with connecting metal members, providing both a fluid-flow channel and prime and extended surfaces, Bejan et al. [7] and Incropera et al. [8].

An arrangement is called a stack or sandwich, where heat can enter a stack through either or both end plates, Bejan et al. [7], while a pair of cores can be arranged as components of a two-fluid heat exchanger in a cross-flow arrangement, where fluids enter alternate cores from separate headers at right angles to each other and leave through separate headers at opposite ends of the heat exchanger. Here, separation plate spacing need not to be the same for both fluids, nor need the cores for both fluids contain the same numbers or kinds of fins. These are dictated by the allowable pressure drops for both fluids and the resulting heat transfer coefficients. When one coefficient is quite large compared with the other, it is entirely permissible to have no extended surface in the alternate cores through which the fluid with the higher coefficient travels, Bejan et al. [7]. Compact heat exchangers may be classified by types of the employed compact elements. These include; circular and flattened circular tubes, tubular surfaces, surfaces with flow normal to banks of smooth tubes, plate-fin surfaces, finned-tube surfaces, and matrix surfaces, Bejan et al. [7]. With the plate-fin construction, it is possible to achieve very large area compactness or heat transfer area per unit volume. Compact heat exchangers with plate-fin surfaces are especially useful where both fluids are gases, Kays and London [13], where they are considered in this paper.

LITERATURE REVIEW

The concept of an air turbine with an external heat source is not new; it dates back to the invention of the gas turbine. Nevertheless, interest in the idea has grown in the last decade; the air turbine is a key component in the externally-fired combined cycle and in the air bottoming cycle. One of the implementations is the use of air bottoming with the topping gas turbine cycle. The air bottoming cycle was proposed to increase the efficiency of the simple-cycle gas turbine units operating on Norwegian oil platforms in view of the CO_2 tax, Bolland et al. [14]. Farrell [15] described a thermodynamic waste heat recovery conversion system, including counterflow heat exchanger with intercooler. The exhaust gases from the gas turbine are recuperated in a heat exchanger by heating air in the secondary air turbine cycle. The heated air expands in the turbine, supplying an additional power. Such a configuration is known as the dual gas turbine combined cycle.

Saghafifar et al. [16] performed a thermo–economic optimization analysis on air bottoming cycles (ABC) with and without intercooler in the bottoming cycle, regarding the effect of the mass flow rate ratio. Ayub et al. [17] carried out thermodynamic analysis including sensitivity analysis for ABC, considering varying mass flow rate ratio, pressure ratio, and effectiveness of integrated heat exchanger. Chmielniak et al. [18] compared the GT-ABC and the combined gas-steam cycle designed for the same class of application, considering the thermodynamic characteristics and preliminary economic analysis.

Khan [19] presented a thermodynamic analysis of an air-bottoming cycle operated by the exhaust gasses of a regenerative gas turbine cycle, utilizing air heat exchangers, considering the effects of the turbine inlet temperature and the mass flow rate ratio. He evaluated the net output, combined thermal efficiency, exergy destruction, and specific fuel consumption. These reported an increase of produced power by 18–30% depending on the number of intercoolers, and an efficiency progress of up to 10%. For example, for the Allison 571 K topping gas turbine, introduction of the air bottoming cycle with two intercoolers led to an increase in power from 5.9 to 7.5 MW and in efficiency from 33.9 to 43.2%. Comparable results were obtained with the General Electric LM2500 topping turbine, Poullikkas [20].

Najjar and Zaamout [21] suggested air bottoming cycle instead of steam and concluded that a combined system with the air-bottoming cycle can improve the gas turbine engine power and efficiency by about 30% and 23%, respectively. Also, an optimum design point for such a system was found to be $R_{ct} = 10$ and $R_{cb} = 2$, with T_{03} chosen at 1400 K where R_{ct} and R_{cb} are the pressure compression ratio of the topping and bottoming cycles, respectively. In addition to the above, the combined system is very much less costly than that using steam by dispensing with boiler, steam turbine, condenser, pumps, water treatment plant, cooling towers, etc. and the needed human resources. Chmielniak et al. [22] presented thermodynamic calculations of the air plate heat exchanger and made a preliminary selection of the device, satisfying the considered economic criteria of financial profitability and cost-effectiveness.

Luchko et al. [23] analyzed the operating parameters of air heat exchanger, revealing insufficient efficiency of its operation in the summer period, recommending changes to the design or to consider a unit with a larger heat transfer surface. Aburwees [24] figured out an increment in output power of 28 MW when GT 13 E2 is selected as a topping cycle and the cycle efficiency increased by 6 %. Tiwari et al. [25] found that the combined system with air bottoming cycle can improve the net power output as well as efficiency by about 35% to 68%. Also, the use of two intercooler considerably improves the performance of ABC and increases the bottoming cycle power output by 16% in the relation to the one intercooler case, meanwhile the net power output and efficiency of combined cycle increases up to 8% and 18% respectively, by adding two intercoolers in ABC in relation to the one intercooler case.

Xian et al. [26] investigated the air heat exchanger thermal performance, considering four kinds of different internal structures. These are simulated by CFD, where the thermal performance is found to be affected by the internal structure, and the inlet velocity was the most important factor. Saghafifar et al. [27] presented an overview for the air bottoming cycles and performed thermo-economic analysis and optimization, evaluating simple and water injected air bottoming cycles against steam bottoming cycles. Sunden [28] presented different methods to analyze and determine the performance of compact heat exchangers, showing the applicability of various computational approaches and their limitations, considering CFD methods based on the finite volume approach.

Price et al. [29] evaluated the heat exchanger structure with multiple different fluid circuits. Khalil et al. [30] studied the performance of different geometry plate fin compact heat exchangers, providing full explanation of comparison methods, identifying the advantages and disadvantages of each type of geometry. Núñez et al. [31] described the heat transfer enhancement via the increase of fluid velocity, adding new heat transfer surfaces, and/or using turbulence promoters, analyzing the relation between velocity, heat transfer coefficient, and pressure drop. Here, the main objectives of this present work and the considered mathematical models for designing and evaluating the dual gas turbine combined air-gas cycle with the desired plate compact heat exchanger are to be introduced next.

STUDY MAIN OBJECTIVES

This paper aims to optimize the desired heat exchangers working within thermal dual gas turbine power generation systems. It studies the characteristics of the anticipated compact heat exchangers to be installed in dual gas combined cycles between the topping turbine exhausted hot gases and the compressed air in the air bottoming cycle. This is conducted to select, determine, and evaluate the characteristics and behavior of the optimum heat exchanger; type, effectiveness, size and material, including the effect of the scaling against pressure loss, flow analysis, running power, and cost and feasibility. The whole power generation system needs to be analyzed using the mathematical presented relations, where different scenarios are to be implemented including; simple air bottoming cycles, cycles with one air intercooler, and cycles with two intercoolers.

THE MATHEMATICAL MODELS

A brief review of the governing thermodynamic main equations is to be introduced, where more details are presented elsewhere, Taha [32]. For a combined of two power cycles, with no intermediate heat loss and supplementary heating, the work output from the lower and top cycles are, Kupprn [11];

$$W_L = \eta_L Q_{HL} \quad \text{and} \quad W_H = \eta_H Q_B \tag{1}$$

Where Q_B is the heat supplied to the upper plant, Q_{HL} is the heat recovered from the top cycle through the heat exchanger, and η_L and η_H are the related efficiencies. Thus, the total dual cycle output power is;

$$W = W_H + W_L = Q_B(\eta_H + \eta_L - \eta_H \eta_L) \tag{2}$$

The thermal efficiency of the combined plant is;

$$\eta_{cp} = W/Q_B = \eta_H + \eta_L - \eta_H \eta_L \tag{3}$$

The turbine inlet temperature is usually determined by the limitations of the high-temperature turbine blade material. Special metals or ceramics are usually selected for their ability to withstand both high stress at elevated temperature and erosion and corrosion caused by undesirable components of the fuel, Kreith et al. [9]. As shown in Figures (1 and 2), air enters the compressor at a state defined by T_1 and p_1, where the compressor exit pressure, p_2.

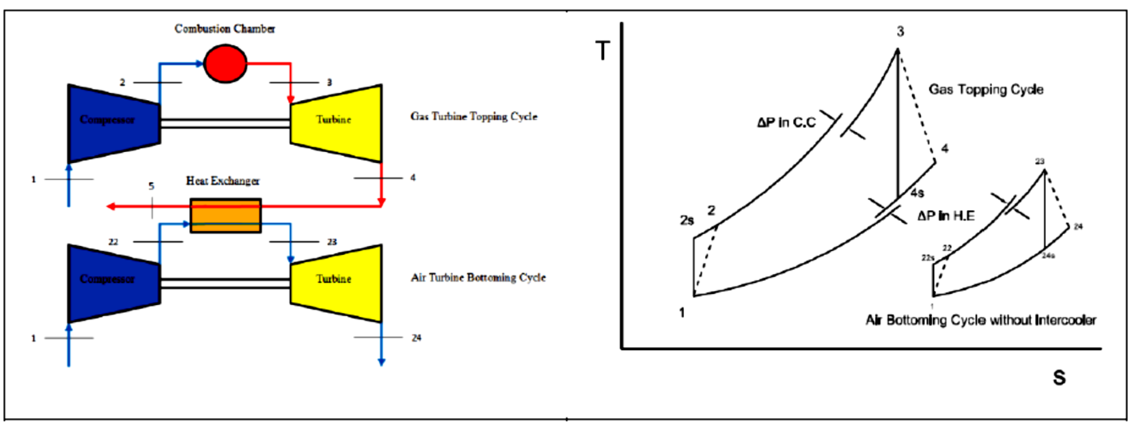

Figure 1: Combined Gas Turbine with Simple Air Bottoming Cycle and T-s diagram.

Referring to the isentropic process, the ideal compressor outlet isentropic temperature is T2s, while the compressor isentropic efficiency is the ratio of the compressor isentropic work to the actual compressor work. Here, the steady-state steady-flow energy equation is employed to obtain expressions for the actual compressor outlet temperature T_2. Then, the specific work required for the top cycle compressor, w_{ct}, is given by [33];

$$w_{ct} = c_{pg} T_1 (1 - R_{ct}{}^{(k-1)/k})/\eta_{ct} \tag{4}$$

Where c_{pg} is the combusted gas specific heat at constant pressure and R_{ct} is the topping compressor pressure ratio.

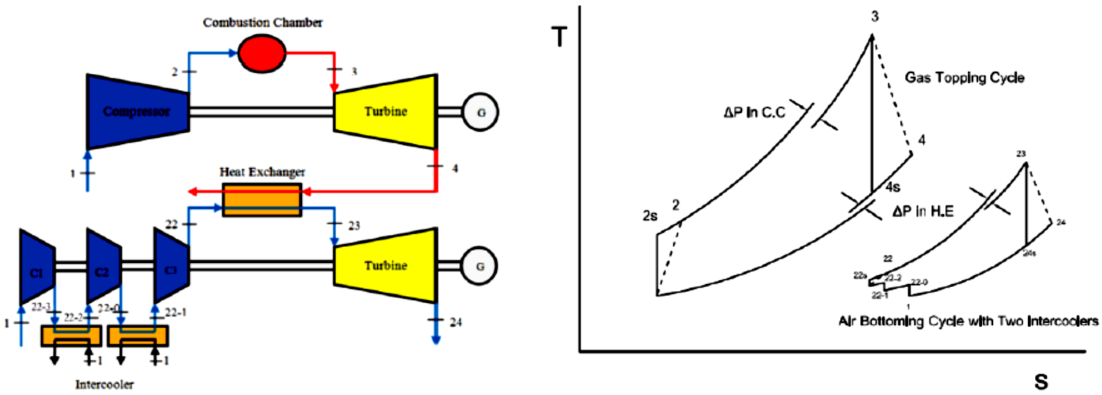

Figure 2: Combined Gas Turbine-Two Intercooler Air Bottoming Cycle with T-s diagram.

The air leaves the compressor at an elevated pressure and temperature, where it enters the combustion chamber. The combustion process raises the combustion gas temperature to the turbine inlet temperature T_3. Referring to the Air Standard Analysis, a fixed value of the combustor fractional pressure loss, fpl, 0.05 or 5%, may be used to account for the burner pressure losses, Kreith et al. [9]. Regarding the turbine inlet pressure and the combustion process, the temperature of the combustion gases rises and the rate of heat released by the combustion process may be expressed as [33];

$$Q_a = \dot{m}(1 + f)c_{pg}(T_3 - T_2) \tag{5}$$

Where f is the mass fuel-air ratio. Here, the sum of the air and fuel mass flow rates equals the mass flow rate of the combustion gas. Referring to the pressure drop along the heat exchanger passage with the turbine outlet atmospheric pressure, the isentropic turbine outlet temperature, T_{4s} can be determined. For steady-state steady-flow conditions, the topping turbine specific work can be written as;

$$w_{tt} = \eta_{tt} c_{pg}(T_3 - T_{4s}) \tag{6}$$

Where η_{tt} is the topping cycle turbine isentropic efficiency. The net specific work based on the mass flow rate of the air processed is then given by [32];

$$w_{nt} = w_{tt}(1 + f) + w_{ct} \tag{7}$$

and the net power output of the topping gas turbine is [32];

$$P_{nt} = \dot{m}_a[w_{tt}(1 + f) + w_{ct}] \tag{8}$$

Where w_{tt} and w_{ct} are the specific power for the topping turbine and compressor, respectively, and $\dot{m}_a$ is the air mass flow rate. The topping thermal efficiency is;

$$\eta_{tht} = w_{net}/q_a \tag{9}$$

Where q_a is the specific heat supplied to the topping cycle. The above thermodynamic analysis of the topping gas turbine cycle is also valid for the air bottoming cycle (ABC) taking into account that the combustion chamber is replaced by the heat exchanger, and the cycle working fluid is air. Regarding the bottoming compressor pressure ratio and the compressor inlet atmospheric air pressure, the isentropic compressor outlet temperature, T_{2s}, can be determined, where the compressor isentropic efficiency and the actual compressor outlet temperature can be defined. Then, the specific work required for the bottoming compressor, w_{cb}, could be given as [32];

$$w_{cb} = c_p T_1 (1 - R_{cb}{}^{(k-1)/k})/\eta_{cb} \tag{10}$$

Where c_p is the air specific heat capacity at constant pressure and R_{cb} is the bottoming compressor air pressure ratio. The air at elevated pressure and temperature enters the heat exchanger, where it rises to a temperature, T_{23}. Referring to the air pressure drop ΔP_a across the heat exchanger while the heat exchanger is well insulated, the rate of heat gained by air flow may be expressed as;

$$Q_{he} = \dot{m}_a c_p [T_{23} - T_{22}] = \dot{m}_g c_{pg} [T_4 - T_5] \tag{11}$$

Employing the isentropic process model with the steady-state steady-flow condition, the bottom turbine specific work can be deduced as;

$$w_{tb} = c_p [T_{23} - T_{24}] = \eta_{tb} c_p [T_{23} - T_{24s}] \tag{12}$$

Where η_{tb} is the bottoming turbine isentropic efficiency. Now, the net specific work of the bottoming gas turbine is given by;

$$w_{nb} = w_{tb} + w_{cb} \tag{13}$$

With a bottoming thermal efficiency of;

$$\eta_{tbt} = w_{nb}/q_{he} \tag{14}$$

Where q_{he} is the specific heat gained by the bottoming cycle. Integrating, the overall performance of the combined dual cycle can be presented. The net plant specific output work is;

$$w_n = w_{nt} + w_{nb} \tag{15}$$

With an overall plant efficiency of;

$$\eta_{th} = w_n/q_a \tag{16}$$

Now, let us see in some details regarding the thermal heat exchanger performance model for the considered compact heat exchanger, based on a number of assumptions, Kaikko [34]. These includes; steady-state steady-flow conditions, negligible heat transfer losses, no phase changes occur, the heat transfer coefficients are fixed, and uniform velocity and temperature over the flow ports cross sections. Referring to the two general types of problems, this study concerns the heat exchanger design problem, where the complete operating parameters are given and the surface area requirements are to be specified after choosing a surface type and a flow arrangement, where the ε-NTU method is suitable with the exchanger heat transfer effectiveness of [13];

$$\varepsilon = \frac{C_h(T_{h,in}-T_{h,out})}{C_{min}(T_{h,in}-T_{c,in})} = \frac{C_c(T_{c,out}-T_{c,in})}{C_{min}(T_{h,in}-T_{c,in})} \tag{17}$$

and the number of transfer units NTU is;

$$\mathrm{NTU} = AU/c_{min} \tag{18}$$

Where U is the overall conductance for heat transfer, W/(m^2.K), A is the surface area on which U is based, with capacity-Rate ratio of;

$$C^* = C_{min}/C_{max} \tag{19}$$

Or generally, ε can be expressed as function of;

$$\varepsilon = \emptyset(\mathrm{NTU}, C_{min}/C_{max}, \text{flow arrangements})$$

Where C_{min} and C_{max} are the smallest and the largest of the two magnitudes of C_h and C_c. Referring to the available flow arrangement; counter flow, parallel flow, cross flow, parallel counter flow, or combination of these basic arrangements; the thermal resistances are [13];

$$\frac{1}{U_h} = \frac{1}{(\eta_o h)_h} + \frac{1}{(\eta_o h_f)_h} + \frac{\alpha_h/\alpha_c}{(\eta_o h_f)_c} + \frac{\alpha_h/\alpha_c}{(\eta_o h)_c} \tag{20}$$

$$\frac{1}{U_c} = \frac{1}{(\eta_o h)_c} + \frac{1}{(\eta_o h_f)_c} + \frac{\alpha_h/\alpha_c}{(\eta_o h_f)_h} + \frac{\alpha_h/\alpha_c}{(\eta_o h)_h} \tag{21}$$

Where the subscripts h and c denote the hot and cold fluid sides, respectively, and the subscript f denotes the fouling or scale. α is the ratio of the total heat transfer area on one fluid side of the heat exchanger to the total volume of the heat exchanger, α =A/V, m^2/m^3. η_o is the extended surface efficiency on one fluid side of the extended surface heat exchanger, h is the heat transfer coefficient, W/m^2.K, G is the mass velocity, kg/m^2.s, and Pr is the Prandtl number. The ε -NTU relations can be stated according to the flow arrangement as follows; Counter-flow [13] and [35]:

$$\varepsilon = \frac{1-e^{-\mathrm{NTU}(1-C^*)}}{1-C^* e^{-\mathrm{NTU}(1-C^*)}} \tag{22}$$

$$\mathrm{NTU} = \frac{1}{C^*-1}\ln\left(\frac{\varepsilon-1}{\varepsilon C^*-1}\right) \tag{23}$$

and for the cross-flow, both fluids unmixed [35];

$$\varepsilon = 1 - e^{\left[\frac{e^{-\mathrm{NTU}^{0.78}C^*}-1}{\mathrm{NTU}^{-0.22}C^*}\right]} \tag{24}$$

Noting that the NTU is a function of ε leading to an implicit equation, that has to be solved numerically. For other relations regarding different heat exchanger arrangements are available elsewhere, Bejan et al. [7], Kays and London [13], and Kays et al. [35]. The pressure drop along the heat exchanger has a significant importance since it extremely affects the fluid pumping power and consequently, the operating running cost. The fluid pressure drop is associated with the entrance and exist effects and fluid friction along the fluid flow passage. The fluid pressure drop has a direct relationship with the exchanger heat transfer, operation, size, mechanical characteristics, and other factors, including economic considerations, Shah et al. [36].

According to Kays and London [13], the pressure drop for the compact heat exchanger can be computed by an equation model. They have introduced heat transfer and flow friction data for approximately 120 surfaces and plotted entrance and exit loss coefficients for plate fin cores and rectangular passages. An optimization procedure could be conducted to select the most suitable heat exchanger that meets the thermal, pressure drop and cost requirements. As well known, many different optimization criteria can be employed, defining the objective function and constraints in the desired design optimization process, where a large number of design variables could be associated with the heat exchanger design.

Here, the heat exchanger is a part of the system, where it could be optimized based on the system objective function by varying pertinent exchanger design variables as well as the system variables in the optimization routine, Shah et al. [36]. In the present sizing problem, the specified pressure drops are the only constraints imposed on the design. The objective of that problem is to optimize the core dimensions to meet the heat transfer required for the specified pressure drops. The power production field is one of the applications that heat exchangers are designed. Referring to Söylemez [37] and Yogesh [38], the net amount of the economic value of the energy savings for the heat recovery plant could be placed as;

$$S = P_1 C_E Q - P_2 C_A A \tag{25}$$

$$Q = \varepsilon(\dot{m}c_p)_{min} \Delta T_{max} \Delta t \tag{26}$$

Where Q is the amount of the annual total heat energy saved by the heat exchanger, [J], C_E is the present price of the energy, [USD/J], C_A is the area dependent first cost of the heat exchanger, [USD/m^2], A is the area of the heat exchanger, [m^2], ΔT_{max} is the maximum temperature deferential in the heat exchanger, [K], and Δt is the annual operation time of the heat exchanger, [s]. P_1 is the ratio of total life cycle net savings of the heat recovery system to the first year's saving, can be given by [32];

$$P_1 = \frac{1}{d-i}\left[1 - \left(\frac{1+i}{1+d}\right)^N\right] \tag{27}$$

Where i is the real fuel price rate, d is the real market interest rate, N is the technical life, [years], P_2 is the ratio of the total life cycle cost of the heat recovery system to its initial cost [37].

$$P_2 = 1 + P_1 M_s - R_v(1+d)^{-N} \tag{28}$$

Where M_S is the ratio of the annual maintenance and operational cost to the original initial cost and R_V is the ratio of the resale salvage value to the initial cost.

METHODOLOGY

The air bottoming cycles are introduced to investigate the effect of the considered desired heat exchangers and compressor pressure ratios on the thermal cycle performance with different scenarios. Governing mathematical models are introduced above with developed performance data for the expected nature of the studied huge compact heat exchangers through curve fitting processes to the available traditional size published data. Work is done on the transformation of the theory into an applicable approach for the evaluation, analysis, and design problems. The sequence of calculations includes the processes of input fluid thermophysical properties, characteristics of the considered combined cycle, computing the fluid mass velocity based on the minimum free area and flow Reynolds number. Selection of the surface basic data, determining the pressure drop and fin efficiency, leading to find out the desired ϵ-NTU [32].

The implemented methodology is to achieve benefit from the available programming tools to ease the calculation processes and consequently achieve a reasonable optimization judgment. A computer program is developed using Microsoft Visual Studio.Net 2008 programming language to facilitate the sizing and optimizing calculations. The programming source code is presented elsewhere, Taha [32]. The program procedure has been built upon the idea of increasing the efficiency associated with employing the heat exchanger between the topping and bottoming cycles. Once the desired combined cycle efficiency is specified, then the whole cycle parameters including the heat exchanger effectiveness can be easily determined. As the heat exchanger effectiveness is determined, the NTU parameter can also be calculated according to the selected counter-flow and unmixed fluids cross-flow arrangements, where the desired heat surface area could be determined.

CASE STUDY

Dual gas turbine combined cycle is considered with Westinghouse 501 gas turbine as a topping gas cycle, meanwhile Westinghouse W301 as a bottoming air cycle, while transporting 435 kg/s flue gases and 199 kg/s air, respectively. Table (1) summarizes the specifications of both turbines, where W301 and W501 produce 32.2 and 160 MW, respectively, Bathie [6], Cohen et al. [39], and Horlock et al. [40].

Table 1: Specifications of Westinghouse 501 and W301 gas turbines [6] and [40].

	Westinghouse W301	Westinghouse W501
Power (MW)	32.2	160
Thermal Efficiency	-	35.6
Pressure Ratio	6.8	14.6
Turbine Inlet Temp. (K)	-	1533
Air flow (kg/s)	198.67 (438 lb/s)	435
Exhaust Temp. (^{o}C)	426.67 (800 ^{o}F)	584

The properties of the atmospheric standard air conditions are applied. A number of other properties and operating conditions for both cycles regarding air and flue gases are introduced in Table (2).

Table 2: The Considered characteristics and operating conditions for the cycle components [32].

Compressor Inlet Temp. [K]	298	Turbine Inlet Temp. [K]	1533
Compressor Inlet Pressure [Bar]	1.013	Turbine Isentropic Eff.	0.9
Compressor Isentropic Eff.	0.86	k for gas	1.33
Compressor Compression Ratio	14.6	cpg, [kJ/kg.K]	1.140
k for air	1.4	ṁg, [kg/s]	450
cpa, [kJ/kg.K]	1.005	Air bottoming cycle, ṁa, [kg/s]	198.7
ṁ a [kg/s]	435	Bottoming compression ratio	6.8
Combustor fraction pressure loss	0.04	Bottoming Turbine Isen. Eff.	0.89
Heat exchanger Pressure drop, gas side [%]	3		
Heat exchanger Pressure drop, air side [%]	3		

RESULTS AND DISCUSSIONS

Data Curve Fittings

The available mathematical relations are implicit algebraic equation in the form of NTU = $f(\varepsilon)$ for unmixed fluids cross-flow case, that imposes the use of the numerical technique for the solution. This needs a curve fitting for the published tabulated data given by Kays and London [13], where a new correlation relationship is built according to the following form Taha [32];

$$\mathrm{NTU} = \varepsilon + (4C^{*} + 1)\varepsilon^{3} + (C^{*3} + 1)^{4}\varepsilon^{8} + (8C^{*2} + 1)^{2}\varepsilon^{18} + (20C^{*} + 2.5)\varepsilon^{90} \qquad (29)$$

This curve fitting procedure has been carried out using RJS GraphSoftware, version 3.90.10, with an error analysis and a comparison with the published tabulated data, Taha [32], as indicated in Figure (3), where a very close agreement is achieved. Other curve fittings of experimental data, introduced by Kays and London [13], have been done and verified; the friction and Colburn factors, with Reynolds number, where SigmaGraph package was employed [32], related to Figure (4), where both results coincide.

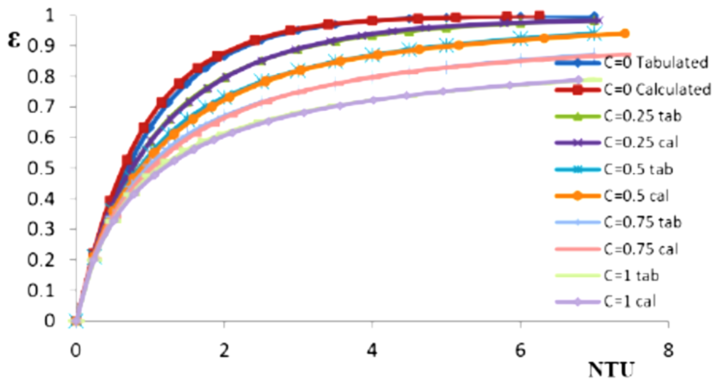

Figure 3: The published tabulated NTU and the new correlation calculated NTU for unmixed fluids cross-flow arrangements

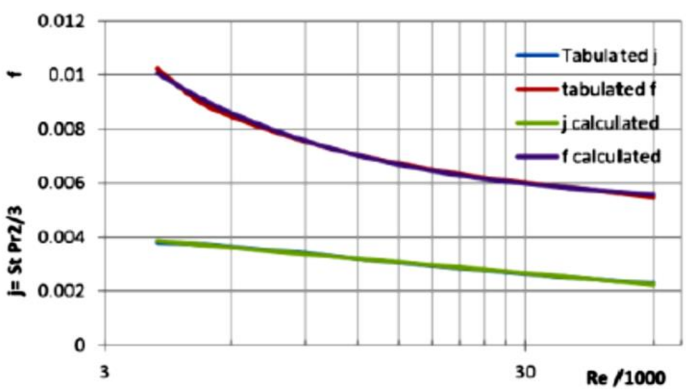

Figure 4: The friction and Colburn factors with Reynolds Number for Plain Plate-fin 2.0 heat exchangers.

Also, the relation between the contraction and expansion loss coefficients with the ratio of free-flow area to frontal area is determined. The gas specific heat and the dynamic viscosity are modeled regarding the effects of the applied high temperatures. Then, the steps of sizing the counter-flow and cross-flow heat exchangers, stated in the literature, Shah et al. [36], have been followed and interpreted to developed Microsoft Visual Studio.Net 2008 routines, Taha [32].

Ntu -Effectiveness Relationships

The obtained results show the expected trend, a linear relation among counter-flow heat exchanger effectiveness and plant power cycle efficiency as introduced in Figure (5), where the efficiency reaches 60% as the effectiveness goes towards 1.0, in a rate of each 0.1 effectiveness improvement gives 1.25 % rise in the efficiency. Here in calculations, the cycle efficiency was the input and the heat exchanger effectiveness is the output. On the other hand, the cycle efficiency rises as the NTU increases to a certain limit, where the curve leans toward the horizontal, leading to an estimated optimum value for the NTU beyond which there is no benefit gained from increasing the NTU. Figure (6) shows this relation for both counter-flow and cross-flow arrangements, where the plant efficiency with the counter-flow heat exchangers is a little better than that with cross-flow arrangements, where they reached 64 and 63%, respectively, with a NTU of above 5.0.

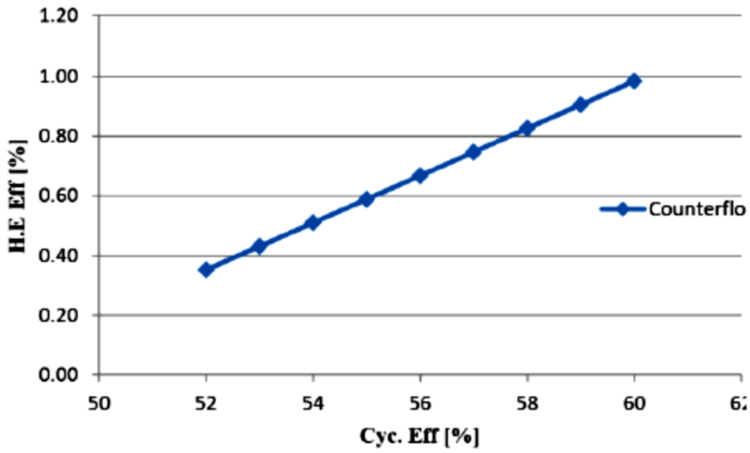

Figure 5: Variation of Heat Exchanger Effectiveness with Combined Cycle Efficiency

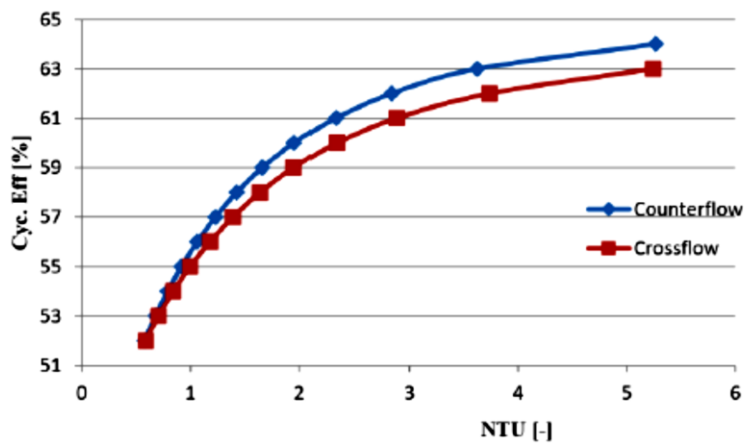

Figure 6: Variation of the Combined Cycle Efficiency with NTU, Plain plate-fin surface 2.0, no intercooler

As for the effect of heat exchanger arrangement, the obtained results show that the core dimensions in the counter-flow arrangement is smaller than those in the cross-flow arrangement as indicated in Figure (7). Here, the NTU in the counter-flow is smaller than that for the cross-flow for a given effectiveness or efficiency. This becomes more visible as the desired effectiveness or efficiency improves, leading to have smaller volume and less weight for the cross-flow heat exchangers. Here, the considered material is not so significant parameter as we will see later on.

Figures (8 and 9) show the effect of heat transfer surface configuration styles on the size of the heat exchanger and consequently on the plant cycle performance for both cross-flow and counter-flow arrangements, respectively. It is clearly found that the strip-fin plate-fin surface geometry gives higher efficiency compared with those when louvered plate-fin surface and plain plate-fin surface geometries are employed with the same heat exchanger volume.

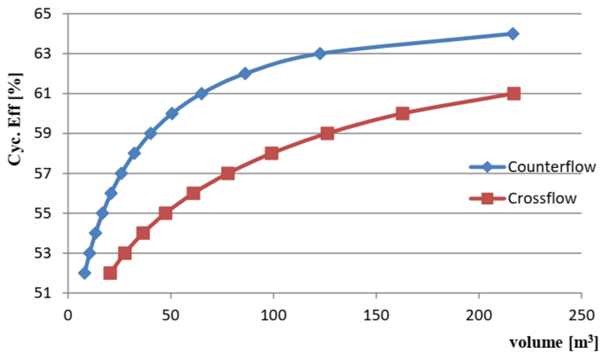

Figure 7: The Combined Cycle Efficiency with H.E. Volume for two flow arrangements, Plain plate-fin surface 2.0, one intercooler.

Ignoring the applicability of the heat exchanger different dimensions, it's obvious to see from the Figure, that the plain plate-fin surface heat exchangers don't reach the semi-optimum volume rapidly with the efficiency for both arrangements. To achieve a plant cycle efficiency of 57%, around 150 and 50 m^3 plain plate-fin heat exchanger sizes are needed for cross-flow and counter-flow arrangements, respectively. While, for the same efficiency, much less volumes of 25 and 10 m^3 for louvered plate-fin heat exchangers are required. This could be partially due to the boundary-layer separation advantage, where the fins with very short flow-lengths, have high heat transfer coefficients, Taha [32].

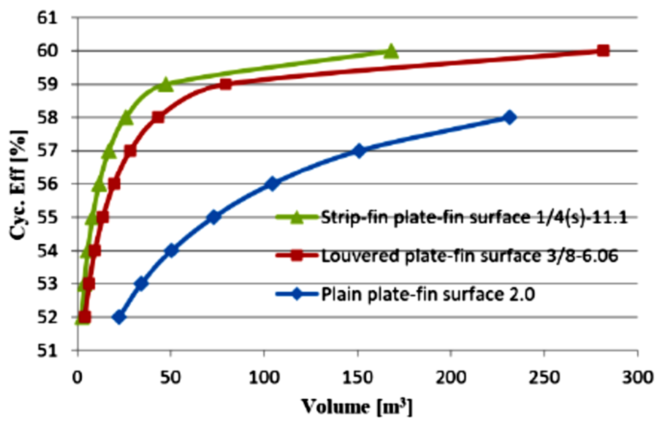

Figure 8: The Combined Cycle Efficiency with H.E. Volume for cross-flow arrangement with different surface configurations, no intercooler.

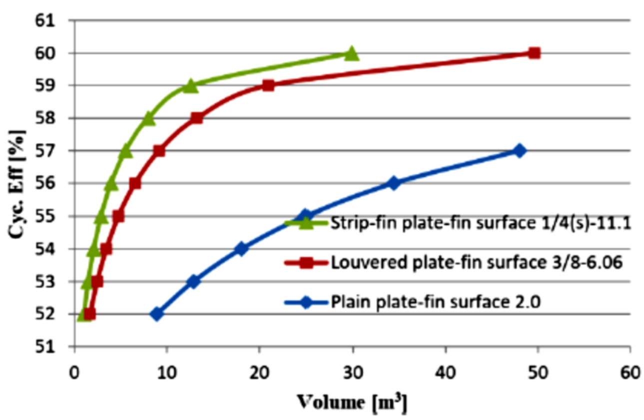

Figure 9: The Combined Cycle Efficiency with H.E. Volume for counter-flow arrangement with different surface configurations, no intercooler.

Heat Exchanger Sheet Metal Role

Figures (10 and 11) show the relationship between the plant cycle thermal efficiency and the heat exchanger size for the counter-flow and cross-flow arrangements, with four common utilized sheet metals. These results confirm that the employed material type has no significant effect on the cycle thermal efficiency for almost every heat exchanger size. There are little variations that appear at small heat exchange sizes. Here in Figure (11), you may see that the volume is so exaggerated to see the whole story!

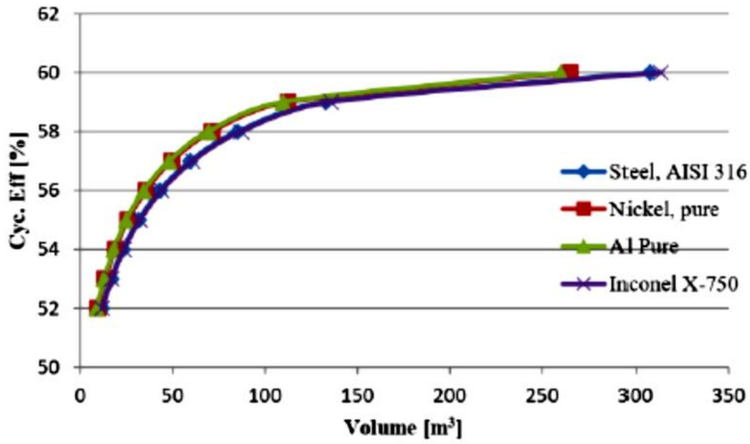

Figure 10: The Combined Cycle Efficiency with H.E. Volume for cross-flow arrangement with different wall materials

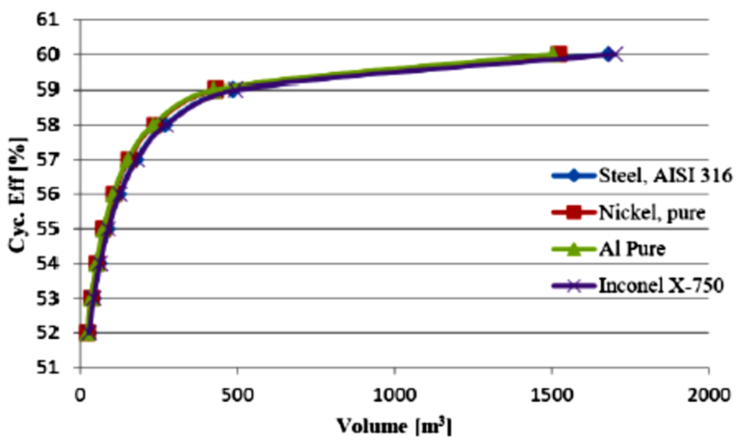

Figure 11: The Combined Cycle Efficiency with H.E. Volume for counter-flow arrangement with different wall materials.

Since the power plant is dealing with large mass flow rates associated with very compact surfaces, the resulting design is expected to involve very up normal sizes and shapes, leading to have no effect due to the type of utilized material, however, the choice will have consequences on both cost and weight.

Plant Energy Savings

The saving in energy cost is quite significant for various thermal systems and it may represent an indicative balance of the overall efficiency of the system when a heat exchanger is being optimized. The published parametric values are used here to determine the related economic money savings, Söylemez [37]. The considered values are; d = 8%, C_E = 1.5 x 10-9 USD/J, C_A = 90 USD/m^2, N = 5 years, where the remaining parameters are taken as; i = 7%, Ms = 0.024, Rv = 0.2, and Δt = 10 x 20 x 12 x 3600 s, corresponding to working hours per day and the number of working days per month. Regarding Plain Plate-Fin Surface 2.00, counter-flow heat exchangers, Figure (12) shows the relationship between the net energy savings in Millions of US dollars with the heat transfer area of the three cases related to the intercooler employments. At the start, as the surface area advances, the savings grow up to a certain maximum peak value at which the optimum heat exchanger area could be determined. Beyond this reflection point, an additional heat exchanger area will not be a cost-effective decision. At the optimum line, the net savings grow up to 30 and 54%, for plants with one and two intercoolers, respectively, based on the simple case with 2.7 MUSD.

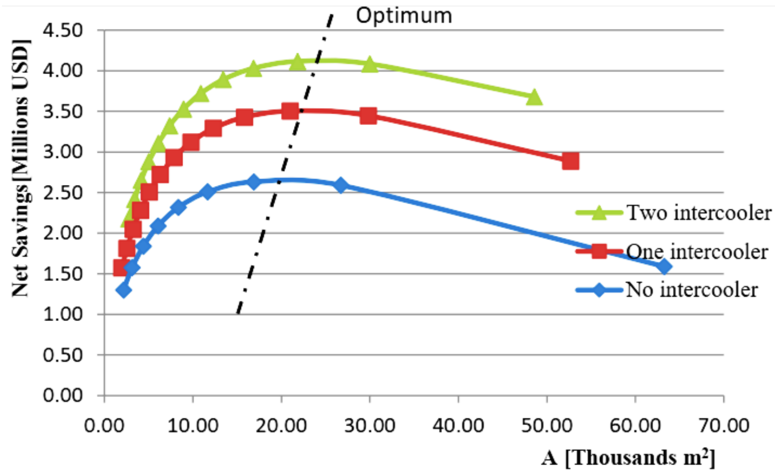

Figure 12: Variation of net savings with area for Plain Plate-Fin Surface 2.00, counter-flow arrangement.

Figure (13) introduces the variation of the plant net savings with the plant Cycle Efficiency for the Plain Plate-Fin Surface 2.00, counter-flow arrangement. It is obvious to have growing savings, for simple cycles or cycles with intercooler(s), as the plant efficiency rises, however, not for all! Here, there are reflection points where the maximum savings reached at optimum efficiencies. Meanwhile, Figure (14) shows the effect of different surface configurations of counter-flow heat exchangers in simple power plant cycles. The strip-fin plate-fin surface gives an optimum savings value of 3.1 MUSD at an efficiency of around 59%.

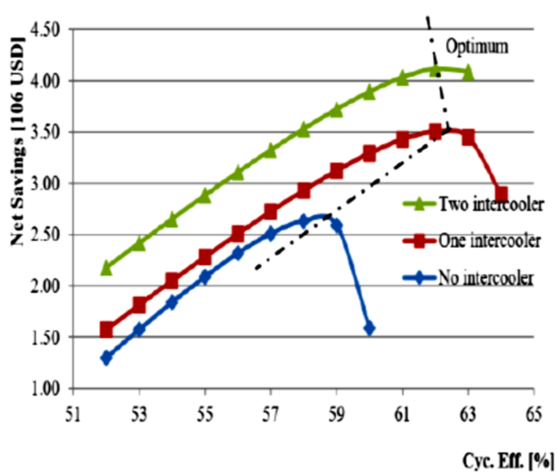

Figure 13: Net Savings with Cycle Efficiency for Plain Plate-Fin Surface 2.00, counter flow arrangement.

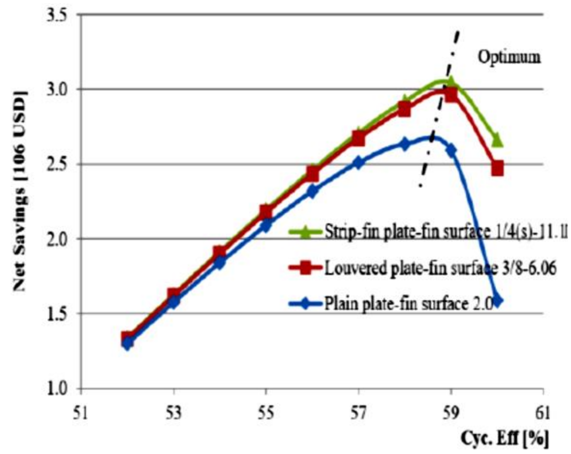

Figure 14: Net Savings with Cycle Efficiency for counter-flow arrangement with no intercooler.

For more details, Figure (15) presents the net energy saving trends with the heat exchanger effectiveness for the Plain Plate-Fin Surface 2.00, counter-flow arrangement, considering the three intercooler cases. The performance is in agreement with the expected behavior presented above in Figure (14), consequently both effects, the plant efficiency and heat exchanger effectiveness on the net savings, are similar, where the same maximum savings could be accomplished.

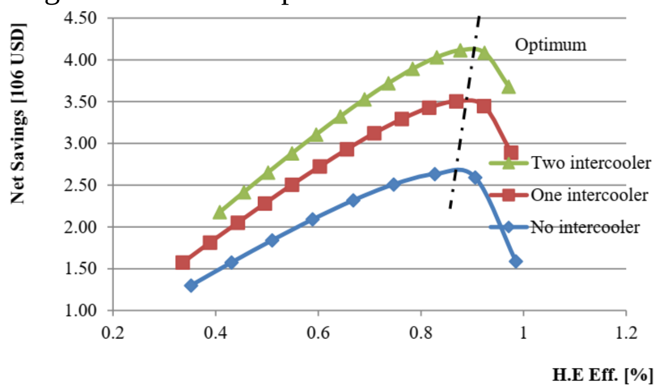

Figure 15: Net Savings with H.E Effectiveness for Plain Plate-Fin Surface 2.00, counter flow arrangement.

Sizing Heat Exchanger

The solution to the sizing problem in general is related to a couple of constraints in addition to keep low pressure loss, whereas the objective of the design is to minimize the weight, volume, heat-transfer surface area, or other considerations, while meeting the required heat transfer target. This scenario is worked on and is achieved by heat exchanger optimization, where the process concerns determining the conditions, that give the minimum (or maximum) of the objective function, Kupprn [11] and Frangopoulos [41]. By using the above present software package, different surface configurations, flow arrangements, and wall material types can be considered to obtain desired parametric ranges of the heat transfer rate, output temperatures, effectiveness, size, weight, etc. Through the deep evaluation and keen judgment of the obtained outcomes, the optimum heat exchanger could be specified

Table (3) presents a selected sample of the obtained characteristics for the Counter-flow arrangement heat exchangers for three different heat surface configurations. By investigation, the heat exchanger dimensions for the Plain plate-fin surface 2.0, Counter-flow heat exchanger, seems to represent the only favorable and applicable choice due to the unacceptable dimensions for the other two alternatives. The Plain plate-fin heat exchangers with two intercoolers in the cycle, with dimensions of 1.77 m x 5.03 m x 10.06 m, presented in the blue highlighted row, seems to be the most acceptable one, as it is related to the highest energy savings, highest efficiency, and highest effectiveness. On the contrary, the weight is high which is a disadvantage and could be resulted regarding the material initial cost. Here, the selected optimum design, generally, doesn't satisfy all of the requirements, where one should look for the best quality or performance per unit cost, with acceptable safe environmental effects, Frangopoulos [41].

Table 3: A sample of the Obtained characteristics for the Counter-flow arrangement heat exchangers.

Surface Configuration	No. of Intercoolers	η [%]	ε [%]	NTU	L [m]	W [m]	H [m]	Weight [kg]	Net Savings [USD]
Plain plate-fin surface 2.0	0	58	82.7	2.299	1.439	4.9110	9.8219	105,132.91	2,632,584.00
	1	62	86.90	2.739	1.717	5.0133	10.026	130,703.61	3,503,494.00
	2	62	87.70	2.837	1.773	5.0288	10.058	135,869.11	4,115,645.00
Louvered plate-fin surface 3/8-6.06	0	59	90.60	3.275	0.360	5.397	10.793	32,080.00	2,963,189.00
	1	63	92.30	3.594	0.402	5.397	10.793	35,859.00	3,863,595.00
	2	63	92.40	3.625	0.407	5.377	10.754	36,024.00	4,503,418.00
Strip-fin plate-fin surface 1/4(s)-11.1	0	59	90.60	3.275	0.215	5.417	10.833	19,431.00	3,043,175.00
	1	63	92.00	3.59	0.24	5.42	10.83	21,715.00	3,953,114.00
	2	63	92.40	3.625	0.243	5.397	10.794	21,815.00	4,593,362.00

CONCLUSIONS AND RECOMMENDATIONS

In this paper, a comprehensive assessment is made of compact heat exchangers proposed in dual gas turbines. Starting with a brief description of dual gas turbine power cycles followed by the role of the desired heat exchangers employed, including presentation of different thermoeconomic mathematical models. A software is built based on the Microsoft Visual Studio.Net 2008 language, to conduct the thermoeconomic behavior for the combined gas cycles under different thermophysical, geometrical and/or operating conditions. An optimization procedure is carried out for the compact heat exchangers, including the heat exchanger type, size, material, weight and cost analyses.

For the mentioned specified conditions, the heat exchanger size is determined for several scenarios, including simple, with one, or with two air intercoolers, counter or cross-flow arrangements, and different selected wall materials. The obtained outcomes seem to be in agreement with the expected manners of the compact heat exchangers working within such defined conditions. The cost wise is playing a key role in the optimization process, and hence the net amount of the economic value of the energy savings, by implementing the heat exchanger, is computed to verify the feasibility of the overall system.

There is a linear relation among counter-flow heat exchanger effectiveness and plant power cycle efficiency. The plant efficiency with the counter-flow heat exchangers is higher than that with cross-flow arrangements, where to achieve a plant cycle efficiency of 57%, around 150 and 50 m^3 plain plate-fin heat exchanger sizes are needed for cross-flow and counter-flow arrangements, respectively. The paper confirms that the employed material type has no significant effect on the cycle thermal efficiency for large heat exchanger sizes. Based on the simple case with 2.7 MUSD, for the Plain Plate counter-flow arrangement, the net savings grow up to 30 and 54%, for plants with one and two intercoolers, respectively. Here, the plant efficiency and heat exchanger effectiveness effects on the net savings, are similar, with same maximum savings. This with two intercoolers in the cycle, with dimensions of 1.77 m x 5.03 m x 10.06 m, is the most acceptable one, with the highest energy savings, efficiency, and effectiveness.

This work could be extended to cover the study of the heat exchanger layouts by splitting the heat exchanger ensued into a number of separate smaller units to be more realistic and applicable. The work could be prolonged to evaluate, analyze and design regenerate and reheat thermal power cycles, where parametric and exergoeconomic studies could be conducted.

NOMENCLATURE AND ABBREVIATIONS

A	Total heat transfer surface area	m^2
C	Flow stream heat capacity rate	W/K
C*	Ratio of heat capacity rates	
c_p	Specific heat of fluid at constant pressure	J/kg.K
Cmax	Maximum of Cc and Ch	W/K
Cmin	Minimum of Cc and Ch	W/K
C_A	Area dependent first cost	USD/m^2
C_E	Present price of energy	USD/J
d	Interest rate	
G	Fluid mass velocity based on the minimum free area	kg/m^2.s
h	Heat transfer coefficient	W/m^2.K
i	Energy price rate	
j	Colburn factor	
K	Pressure loss coefficient	
k	Isentropic exponent	
L	Fluid flow length on one side of an exchanger	m
Lf	Fin flow length on one side of a heat exchanger	m
$\dot{m}$	Fluid mass flow rate	kg/s
MS	Ratio of annual running cost to the initial cost	
N	Technical life	years
NTU	Number of transfer units	
Pr	Prandtl number	
ΔP	Fluid static pressure loss	bar
Q	Annual total heat transfer	J
Re	Reynolds number	
R_V	Ratio of resale value into first cost	
S	Net present value of energy savings	USD
T	Fluid temperature	ºC
U	Overall heat transfer coefficient	W/m^2.K
V	Heat exchanger total volume	m^3
Δt	Annual total operation time	s
ε	Heat Exchanger effectiveness	
α	Ratio of total heat transfer area to the total volume	m^2/m^3
β	Heat transfer surface area density	
δ	Fin thickness	m
η	Fin efficiency	
ηo	Extended surface efficiency on one fluid side	
μ	Fluid dynamic viscosity	Pa .s
ρ	Fluid density	kg/m^3
σ	Ratio of free flow area to frontal area	

REFERENCES

[1] Marie Anheden, “Analysis of Gas Turbine Systems for Sustainable Energy Conversion”, PhD Thesis, Royal institute of technology, Stockholm, Sweden, 2000.

[2] Nina Katharina Hepperle, “Design of a Heat Exchanger for an Intercooled Recuperated Aero Engine”, MSc thesis, Cranfield university, 2007.

[3] Ekin Özgirgin, “Utilization of Natural Gas, Optimization of Cogeneration/Combined Cycle Applications in Campus Environment”, MSc thesis, the middle east technical university, 2004.

[4] R. H. Williams and E. D. Larsont, “Biomass Gasifier Gas Turbine Power Generating Technology”, Biomass and Bioenergy, 10(2-3), 149- 166, 1996.

[5] M. A. Korobitsyn, “New and Advanced Energy Conversion Technologies. Analysis of Cogeneration, Combined and Integrated Cycles”, PhD Thesis, University of Twente, 1998.

[6] William W. Bathie, “Fundamentals of gas turbines”, John Wiley & Sons, 1984.

[7] Bejan, Adrian, and Allan D. Kraus, “Heat Transfer Handbook”, John Wiley & Sons, Inc, 2003.

[8] Incropera, F. P., Dewitt, D. P., “Fundamentals of Heat and Mass Transfer”, John Wiley & Sons, Inc., 1996.

[9] Kreith, F., Boehm, R. F., et al. “Heat and Mass Transfer”, Mechanical Engineering Handbook, Boca Raton: CRC Press LLC, 1999.

[10] Yunus A. Cengel “Heat Transfer a Practical Approach”, McGraw-Hill, 1998.

[11] T. Kupprn, “Heat exchanger Design Handbook”, Marcel Dekker inc., New York Basel, 2000.

[12] Shah, R. K. “Compact Heat Exchangers for Microturbines”, In Micro Gas Turbines, pp. 2.1-2.18, 2005. Educational Notes RTO-EN-AVT-131, Paper 2. Neuilly-sur-Seine, France: RTO.; http://www.rto.nato.int/abstracts.

[13] Kays, W. M. and A. L. London, “Compact Heat Exchangers”, Krieger, 1984.

[14] O. Bolland, M. Forde and B. Hande, “Air Bottoming Cycle: Use of Turbine Waste Heat for Power Generation”, Journal of Engineering for Gas and Power, Vol. 118, 1996.

[15] Farrell, W. M., “Air Cycle Thermodynamic Conversion System”, General Electric Co., Schenectady, NY, United States, 1988.

[16] Mohammad Saghafifar, Andreas Poullikkas, “Thermo–economic optimization of air bottoming cycles”, Journal of Power Technologies 95 (3), 211–220, October 2015.

[17] Abubakr Ayub, Nadeem Sheikh, Rasikh Tariq, Mahabat Khan, “Thermodynamic Optimization of Air Bottoming Cycle for Waste Heat Recovery”, Second International Conference on Energy systems for Sustainable Development, ESSD-2017, Lahore, Islamabad, Pakistan, February 2018.

[18] Tadeusz Chmielniak, Daniel Czaja, Sebastian Lepszy, “A thermodynamic and economic comparative analysis of combined gas-steam and gas turbine air bottoming cycle”, Proceedings Of ECOS 2012 - The 25th International Conference On efficiency, cost, optimization, simulation And Environmental Impact Of Energy Systems, June 26-29, 2012, Perugia, ITALY.

[19] Mohammad Nadeem Khan, “Energy and Exergy Analyses of Regenerative Gas Turbine Air-Bottoming Combined Cycle: Optimum Performance”, May 2020.

[20] Andreas Poullikkas, Review An overview of current and future sustainable gas turbine technologies, Renewable and Sustainable Energy Reviews, 9 (409- 443), 2005.

[21] Y. S. H. Najjar and M. S. Zaamout, “Performance analysis of gas turbine air-bottoming combined system” Energy Convers. Mgmt Vol. 37, No. 4, pp. 399403, 1996

[22] Tadeusz Chmielniak, Daniel Czaja, Sebastian Lepszy, “Selection of the air heat exchanger operating in a gas turbine air bottoming cycle”, Archives of Thermodynamics 34(4), December 2013.

[23] Mihail Luchko, Larisa Fomina, “Air Heat Exchanger Analysis”, Modern Technologies and Scientific and Technological Progress (1):51-52, June 2020.

[24] A. Aburwees, “Air Bottoming Cycles Thermodynamics Analysis”, Master Thesis, Almergib University, 2005-2006.

[25] A. K. Tiwari, Mohammed Islam, M. N. Khan “Thermodynamic Analysis of Combined Cycle Power Plant”, International Journal of Engineering Science and Technology, Vol. 2(4), 480-491, 2010.

[26] Zhaokun Xian, Xiaoxian Tang, Han Mo, “CFD simulation different inner structure of air heat exchanger”, IOP Conference Series Earth and Environmental Science 199(5):052032, December 2018.

[27] Mohammad Saghafifar, Mohamed Gadalla, “A critical assessment of thermo-economic analyses of different air bottoming cycles for waste heat recovery”, International Journal of Energy Research 43(5), November 2018.

[28] Bengt Sunden, “Simulation of compact heat exchanger performance”, International Journal of Numerical Methods for Heat and Fluid Flow 20(5):551-569, June 2010.

[29] Andrew R. Price, Rachid Kaina, Mark C. Garnett, Method and structure for optimizing heat exchanger performance, United states Patent: US8593811B2, November 2013.

[30] Ibrahim Khalil, Ahmad Abu-Heiba, Robert F. Boehm, “Comparison of Plate Fin Compact Heat Exchanger Performance”, Conference: ASME 2008 International Mechanical Engineering Congress and Exposition, January 2008.

[31] Martín Picón Núñez, Jorge Luis García-Castillo, Jorge C. Melo-González, “Heat transfer enhancement technologies for improving heat exchanger performance”, In book: Process Intensification, December 2019.

[32] Taha Abuagela Ellabib, “Optimization of Heat Exchanger in a Dual Gas Turbine Combined Cycle”, Thesis of Master of Science degree in Mechanical Engineering, University of Tripoli, Libya, 2011.

[33] Kenneth C. Weston, “Energy Conversion” - The eBook, http://www.personal.utulsa.edu/~kenneth-weston , 2000.

[34] Juha Kaikko, “Air Bottoming Cycle, an Alternative to Combined Cycles”, Final Report, Avdelningen för Kraft- och Värmeteknologi, Kungliga Tekniska Högskolan, 100 44 STOCKHOLM, 2007.

[35] Kays, W. M. and M. E. Crawford, “Convective Heat and Mass Transfer”, McGraw-Hill, 1993.

[36] Ramesh K. Shah and Dusˇan P. Sekulic, “Fundamentals of Heat Exchanger Design”, John Wiley & Sons, Inc., 2003.

[37] Söylemez M. S. “On the optimum heat exchanger sizing for heat recovery”, Energy Conversion & Management 2000; 41(13):1419-27.

[38] Yogesh Jaluria, “Design and Optimization of Thermal Systems”, CRC Press, Taylor & Francis Group, 2008.

[39] Cohen, H., Rogers, G. F. C., and Saravanamutto, H. I. H., “Gas turbine Theory”, John Wiley & Sons, 1996.

[40] J. H. Horlock, F. R. Eng., F. R. S. “Advanced Gas Turbine Cycles”, Whittle Laboratory Cambridge, UK., 2003.

[41] Christos A. Frangopoulos “Optimization of Energy Systems and Processes”, Report; OPTI_ENERGY, Summer School: Gliwice, Poland, 24. 27, 2003.